ResearchGate

See discussions, stats, and author profiles for this publication at: https://www.researchgate.net/publication/255115121

Kinetic and Electronic Energy Dependence of the Reactions of Sc+ and Ti+ with D2O

ARTICLE *in* THE JOURNAL OF PHYSICAL CHEMISTRY · NOVEMBER 1994

Impact Factor: 2.78 · DOI: 10.1021/j100095a034

CITATIONS
39

READS
6

3 AUTHORS, INCLUDING:

P. B. Armentrout
University of Utah
492 PUBLICATIONS **20,531** CITATIONS

SEE PROFILE

Available from: P. B. Armentrout
Retrieved on: 24 January 2016

Kinetic and Electronic Energy Dependence of the Reactions of Sc^+ and Ti^+ with D_2O

Yu-Min Chen, D. E. Clemmer, and P. B. Armentrout*

Department of Chemistry, University of Utah, Salt Lake City, Utah 84112

Received: June 27, 1994; In Final Form: August 22, 1994[⊗]

The reactions of Sc^+ and Ti^+ with D_2O are studied as a function of translational energy in a guided ion beam tandem mass spectrometer. Both ions react to form three ionic products: MD^+, MO^+, and MOD^+. MO^+ formation occurs exothermically by dehydrogenation of D_2O, even though this reaction is spin forbidden for reaction of ground state M^+ in both systems. In the titanium system, the effect of electronic energy on product formation is probed by varying the conditions used for forming Ti^+. The a^2F state of Ti^+ reacts much more efficiently than the a^4F ground state at forming all three product ions. The relative reaction efficiencies are consistent with a recent study of the reverse reactions of $MO^+ + D_2$ [*J. Phys. Chem.* **1993**, *97*, 544]. State-specific cross sections and the competition between the various products indicate that the reactions occur primarily through a low-spin state of a $D-M^+-OD$ intermediate. Thresholds of the cross sections for endothermic formation of all three product ions are consistent with values calculated by using previously measured bond energies.

Introduction

We have recently determined a fairly detailed picture of the potential energy surfaces and reaction mechanisms for the reactions involved in the conversion of CH_4 to CH_3OH by two transition metal oxide cations (MO^+), CoO^+ and FeO^+, by using a guided ion beam mass spectrometer to study the reactions in both the forward and reverse directions, $MO^+ + CH_4 \leftrightarrow M^+ + CH_3OH$.[1,2] Such studies not only are of fundamental interest in understanding the activation of C−H σ-bonds by transition-metal oxides but also can provide quantitative information regarding the thermodynamics and mechanisms for the catalytic oxidation of methane to methanol. In conjunction with this work, we[1,3] and Schwarz and co-workers[4] have studied the related but simpler $MO^+ + D_2 \leftrightarrow M^+ + D_2O$ reactions for CoO^+ and FeO^+, which help in understanding and confirming the reaction mechanisms and potential energy surfaces for the methane oxidation. We have extended such studies to the activation of D_2 by three early transition-metal oxides, ScO^+, TiO^+, and VO^+,[5] and to state-specific studies of the reactions of D_2O with ground state $V^+(a^5D)$ and excited triplet states of V^+.[6] In the present paper, we report our studies of reaction 1

$$M^+ + D_2O \rightarrow MO^+ + D_2 \qquad (1)$$

for ground state $Sc^+(a^3D)$ and $Ti^+(a^4F)$, as well as the low-lying excited doublet states of Ti^+. By combining the results of this study with our previous work[5] of the reactions of ScO^+ and TiO^+ with D_2, we obtain a more complete picture of the potential energy surfaces for this simple oxidation process.

The oxidations of CH_4 and D_2 by CoO^+ and FeO^+, although thermodynamically favored, are found to be kinetically constrained by an activation barrier in the entrance channel. We have attributed this barrier to a four-centered transition state associated with addition of CH_3-H or D−D across the M^+-O bond,[1−3] and ab initio calculations have confirmed this subsequently.[7] For the reaction of ScO^+ with D_2, however, no barrier is observed experimentally[5] because the overall reaction to form $Sc^+ + D_2O$ is more endothermic (2.1 eV) than the anticipated barrier height (0.5−0.8 eV in the FeO^+ and CoO^+ systems[1,3]). For the reactions of D_2 with two other early transition-metal ions, TiO^+ and VO^+, the relative energetics are comparable to the scandium system, but the thresholds observed for $M^+ + D_2O$ formation were higher than the thermodynamic values. In explaining this observation, we noted that the ground states of $Sc^+(a^3D)$, $Ti^+(a^4F)$, and $V^+(a^5D) + D_2O(^1A_1)$ are all high spin, while the ground states of $ScO^+(^1\Sigma^+)$, $TiO^+(^2\Delta)$, and $VO^+(^3\Sigma^-) + D_2(^1\Sigma_g^+)$ are all low spin. Therefore, the elevated thresholds were attributed to the preferential formation of the excited states of M^+ that conserve spin with the $MO^+ + D_2$ reactants rather than to a barrier to reaction.[5] Differences in the behavior of the three systems were explained by noting that the splitting between the high-spin ground states of M^+ and the low-spin excited states increases from Sc^+ (0.3 eV) to Ti^+ (0.6 eV) to V^+ (1.1 eV). For the $VO^+ + D_2$ reaction system, this hypothesis is consistent with studies of the reverse reaction 1.[6] One specific purpose of the present study is to test this hypothesis in the titanium system by examining reaction 1 and to better understand the differences in the behavior of the scandium, titanium, and vanadium systems.

Aside from the congruent relationship of this system with our previous study of reaction 1 and its reverse for other metal systems, the present work also allows us to gain a fundamental understanding of the activation of O−D bonds. Detailed knowledge of how bonds in small molecules are activated by transition-metal ions is a primary motivation for much of the work in our laboratories. State-specific reaction studies of transition-metal ions with small molecules have provided insight into the electronic requirements for the activation of H−H, C−H, C−C, and N−H bonds by transition metal ions.[8] In the present work, the activation of the O−D bonds of water is examined. Water is isoelectronic (in the sense that the central heavy atom has the same number of valence electrons with the same sp^3 hybridization)[9] to the ammonia and methane molecules. We have previously studied the reactions of Sc^+ and Ti^+ with NH_3[10] and CH_4,[11,12] providing results usefully compared to the present work.

The reaction of Ti^+ with water at thermal energies has been studied by Castleman and co-workers by using a SIDT-LV (selected ion drift tube with laser vaporization source) technique.[13] The only primary reaction product observed was TiO^+, and the rate constant was measured to be $(1.00 \pm 0.02) \times 10^{-10}$ $cm^3\ s^{-1}$. A reaction mechanism, analogous to one given by Freiser and co-workers to explain the reactivity of metal ions with XH_n molecules (where X = C, N, and O),[14] was used to

[⊗] Abstract published in *Advance ACS Abstracts*, October 1, 1994.

0022-3654/94/2098-11490$04.50/0 © 1994 American Chemical Society

rationalize the dehydrogenation process. In this mechanism, an initial step where Ti^+ inserts into the O−H bond to form H−Ti^+−OH is followed by hydrogen migration to form H_2-Ti^+−O, which then loses H_2 to form TiO^+. In contrast, we have suggested that H−M^+−OH species are likely to eliminate H_2 through a four-centered transition state.[6] Studies of reaction 1 at elevated energies may be able to provide insight into which of these mechanisms is operative.

For the reaction of Sc^+ with water, Tilson and Harrison have reported a theoretical study characterizing possible products by using ab initio techniques.[15] Their calculations give the stability and bonding of species such as Sc^+−OH_2, H−Sc^+−OH, (H_2)·ScO^+, Sc^+−OH + H, HSc^+−O + H, and ScO^+ + H_2. Such information is useful in interpreting the experimental results in the present study.

Experimental Section

General Procedures. The guided ion beam instrument on which these experiments were performed has been described in detail previously.[16,17] Sc^+ and Ti^+ ions are produced as described below. The ions are extracted from the source, accelerated, and focused into a magnetic sector momentum analyzer for mass analysis. Mass-selected ions are slowed to a desired kinetic energy and focused into an octopole ion guide that radially traps the ions.[18] The octopole passes through a static gas cell containing the neutral reactant. Gas pressures in the cell are kept low (between 0.06 and 0.15 mTorr) so that multiple ion−molecule collisions are improbable. All results reported here are due to single bimolecular encounters, as verified by pressure-dependent studies. Product and unreacted beam ions are contained in the guide until they drift out of the gas cell where they are focused into a quadrupole mass filter for mass analysis and then detected. Ion intensities are converted to absolute cross sections as described previously.[16] Uncertainties in absolute cross sections are estimated to be ±20% (which includes a 10% error in the pressure measurement). Relative uncertainties are about 5% for cross sections greater than about 2×10^{-18} cm^2 and are limited by statistical counting uncertainties for smaller cross sections.

Laboratory ion energies (lab) are converted to energies in the center-of-mass frame (CM) by using the formula $E_{CM} = E_{lab}m/(m + M)$, where M and m are the ion and neutral reactant masses, respectively. The absolute zero and distribution of the ion kinetic energy are determined by using the octopole beam guide as a retarding potential analyzer.[16] The uncertainty in the absolute energy scale is ±0.05 eV (lab). The distribution of ion energies is nearly Gaussian with average fwhm of about 0.5 eV (lab) for ions produced in the flow tube source and about 0.9 eV (lab) for ions formed by surface ionization or electron impact. The thermal motion of the D_2O gas in the reaction cell has a distribution with a fwhm of $\sim 0.45E_{CM}^{1/2}$ eV.[19] At very low energies, the slower ions in the kinetic energy distribution of the beam are not transmitted through the octopole, resulting in a narrowing of the ion energy distribution. We take advantage of this effect to access very low interaction energies as described previously.[16,20]

Ion Sources. The Sc^+ and Ti^+ ions used in these experiments were produced in a flow tube (FT) ion source, and Ti^+ was also produced by using surface ionization (SI) and electron impact (EI) ion sources. The FT source consists of a 1 m long flow tube and a dc discharge source that is described in detail elsewhere.[17,21] The flow gases used are ~90% He and ~10% Ar maintained at a total pressure of 0.5−0.8 Torr. Metal ions are generated by ~2.5 keV Ar ion impact on a cylindrical rod made of titanium metal or on $ScCl_3$ salt contained in a small (~2 cm^3 capacity) tantalum bowl. The ions are then swept down the flow tube by the He and Ar flow gasses and undergo $\sim 10^5$ collisions with the flow gases. A test reaction of Ti^+ with methane was conducted, and comparison of the result with previous state-specific results for this reaction[11] suggested that trace amounts of high-lying excited state Ti^+ ions can survive these flow conditions. These excited state ions are easily removed by introducing CH_4 to the flow tube about 25 cm downstream of the source at a pressure of ~2 mTorr. The same amount of CH_4 was also introduced into the flow tube when Sc^+ was produced. The comparison of results for the Sc^+ + CH_4 reaction with previous SI results[12] suggests that excited states are quenched to the ground state. On the basis of the methane test results, we believe that these conditions produce Ti^+ and Sc^+ ions mostly in their ground electronic state and assume that the populations of the spin−orbit levels have a Maxwell−Boltzmann distribution at 300 K.

TABLE 1: Electronic States of Sc^+ and Ti^+ and Their Populations

				% population		
ion	state	config	E,[a] eV	SI (2200 K)[b]	EI (30 eV)	
Sc^+	a^3D	$3d^14s$	0.013			
	a^1D	$3d^14s$	0.315			
	a^3F	$3d^2$	0.609			
	b^1D	$3d^2$	1.357			
Ti^+	a^4F	$3d^24s$	0.028	62.50	73(7)[c]	80(3)[e]
	b^4F	$3d^3$	0.135	35.55		0[e]
	a^2F	$3d^24s$	0.593	1.59	9(3),[c] 14(5)[d]	≤18[e]
	a^2D	$3d^24s$	1.082	0.09		≥2[e,f]
	a^2G	$3d^3$	1.124	0.12		
	a^4P	$3d^3$	1.172	0.06		
	a^2P	$3d^3$	1.232	0.02		
	b^4P	$3d^24s$	1.236	0.05		
	Σ states		>0.5 eV	1.95		

[a] Energies are a statistical average over the spin−orbit levels. [b] Maxwell−Boltzmann distribution. [c] Reference 11. [d] Reference 10. [e] Reference 25. [f] This population is for all high-lying states of $3d^24s$ configuration.

In order to produce beams that contain well-known fractions of excited states, Ti^+ was produced by surface ionization (SI). In the SI source, the metal is introduced to the gas phase as $TiCl_4$. The metal halide vapor is directed toward a resistively heated rhenium filament where it decomposes, and the resulting metal atoms are ionized. It is generally assumed that ions produced by SI equilibrate at the temperature of the filament and the state populations are governed by a Maxwell−Boltzmann distribution. The validity of this assumption has been discussed previously[11] and recently verified by van Koppen et al. for Co^+.[22] Table 1 lists the energies and populations of states for Ti^+ produced at the SI temperature used in these experiments. Because all transitions between states in Table 1 are parity forbidden, the radiative lifetimes of the excited states (on the order of seconds long)[23] are expected to be much greater than the flight time between the ionization and reaction regions (10−100 μs). Thus, very few excited ions radiatively relax before reaction.

In order to produce Ti^+ beams that contain large fractions of excited state ions, we also produced Ti^+ ions by using an EI source. We have attempted on several occasions to produce Sc^+ in an EI source but have been unsuccessful because no suitable precursor can be found. In the EI source, 30 eV electrons ionize and dissociate $TiCl_4$ vapor to form Ti^+ and other ions. Because the appearance energy of Ti^+ from $TiCl_4$ is 25.0 eV,[24] it is possible to form significant percentages of excited state ions at an electron energy of 30 eV. The populations of the excited states of Ti^+ formed under these conditions have been studied in our laboratory[10,11] and are listed in Table 1. Kemper and Bowers also have reported the state populations

TABLE 2: Bond Energies at 0 K

bond	D_0, eV	bond	D_0, eV
Sc^+-O	7.14(0.07)[a]	Ti^+-OH	4.82(0.12)[a] 4.90(0.13)[d]
Sc^+-D	2.47(0.09)[b]	Ti^+-OH_2	1.60(0.06),[h] 1.65(0.13),[d] 1.63[e]
Sc^+-OH	5.17(0.09),[a] 4.68[c]	D−D	4.556[i]
Sc^+-OH_2	1.36(0.13),[d] 1.50,[e] 1.57[c]	O−D	4.454(0.003)[i]
Ti^+-O	6.88(0.07)[f]	D−OD	5.212(0.003)[i]
Ti^+-D	2.34(0.11)[g]		

[a] Reference 5. [b] Elkind, J. L.; Sunderlin, L. S.; Armentrout, P. B. *J. Phys. Chem.* **1989**, *93*, 3151. [c] Reference 15. [d] Magnera, T. F.; David, D. E.; Michl, J. *J. Am. Chem. Soc.* **1989**, *111*, 4100. No temperature specified. [e] Reference 37. [f] Clemmer, D. E.; Elkind, J. L.; Aristov, N.; Armentrout, P. B. *J. Chem. Phys.* **1991**, *95*, 3387. [g] Elkind, J. L.; Armentrout, P. B. *Int. J. Mass. Spectrom. Ion Processes* **1988**, *83*, 259. [h] Reference 38. [i] Calculated from heats of formation given by: Gurvich, L. V.; Veyts, I. V.; Alcock, C. B. *Thermodynamic Properties of Individual Substances*, 4th ed.; Hemisphere: New York, 1989; Vol. 1, Part 2.

for Ti^+ produced by EI at 30 eV determined in an ion chromatography study.[25] As shown in Table 1, their population measurements are consistent with our values. In our previous work, we assigned a collective value for the population of ground state a^4F and first excited state b^4F because the two states are too close in energy to be distinguished. Kemper and Bowers found no evidence for the presence of the b^4F state, but it is possible that any b^4F state produced by EI at 30 eV is quenched to the ground state by collisions with the He buffer gas which was maintained at a pressure of 1−5 Torr in their experiment. According to the collision deactivation model proposed by Loh et al.,[26] the potential energy surfaces for the interactions of $Ti^+(a^4F)$ and $Ti^+(b^4F)$ with He should cross. Because the two states have the same spin, the collisional deactivation of the b^4F state to ground state a^4F should be reasonably efficient. In our experiment, the pressure in the EI ion source region was as low as 10^{-5} Torr, such that quenching of the b^4F state is not assured.

Neutral Gas. D_2O was obtained from Cambridge Isotope Laboratories with purity stated as 99.9%. The D_2O was purged with dry N_2 gas before use in order to remove any dissolved oxygen. Residual oxygen is a complication in the present experiments because Sc^+ and Ti^+ react with O_2 to form ScO^+ and TiO^+ very efficiently.[27]

Data Analysis. The energy dependence of the reaction cross sections are modeled by using eq 2,[28]

$$\sigma(E) = \sigma_0(E + E_{int} + E_{el} - E_0)^n/E \qquad (2)$$

where σ_o is a scaling factor, E is the relative kinetic energy, E_{int} is the internal energy of the D_2O reactant (0.039 eV at 305 K, the nominal temperature of the octopole), n is an adjustable parameter, E_0 is the threshold for reaction of the lowest electronic level of the M^+, and E_{el} is the average electronic excitation energy of the metal ions. For ions produced in the FT source, the values of E_{el} at 300 K are 0.009 and 0.018 eV for Sc^+ and Ti^+, respectively. When data obtained for M^+ generated by SI and EI are analyzed, the thresholds are reported as $E_T = E_0 - E_{el}$. Comparison of E_T values with E_0 can then be used to estimate E_{el} and thus which excited states make appreciable contributions to the SI or EI data. Before comparison with the data, eq 2 is convoluted with the kinetic energy distributions of the ion and neutral reactants.[16] The σ_o, n, and E_0 parameters are then optimized by using a nonlinear least-squares analysis to give the best reproduction of the data. Error limits for E_0 are calculated from the range of threshold values for different data sets over a range of acceptable n values and the absolute error in the energy scale.

Due to the attractive interaction between an ion and neutral molecules, there are often no activation barriers in excess of the endothermicity for ion−molecule reactions.[28,29] Thus,

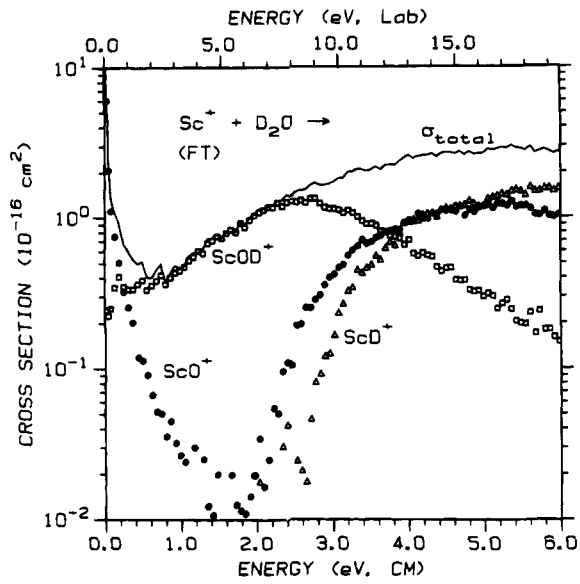

Figure 1. Variation of product cross sections for reaction of D_2O with Sc^+ produced in the flow tube (FT) source as a function of translational energy in the center-of-mass frame (lower scale) and laboratory frame (upper scale). The solid line is the sum of the cross sections for all products.

reaction thresholds measured here are anticipated to equal thermodynamic thresholds, i.e., the energy differences between reactants and products. Because all available energy is accounted for in eq 2, the E_0 thresholds correspond to 0 K values. This assumption can be explicitly tested in the systems studied here because much of the needed thermochemistry is available (Table 2). This thermochemistry is listed with each reaction in the following section.

Results

$Sc^+(a^3D) + D_2O$. Three ionic products, formed in reactions 3−6,

$$Sc^+ + D_2O \rightarrow ScD^+ + OD - 2.74 \pm 0.09 \text{ eV} \qquad (3)$$

$$\rightarrow ScOD^+ + D - 0.04 \pm 0.09 \text{ eV} \qquad (4)$$

$$\rightarrow ScO^+ + D_2 + 2.03 \pm 0.06 \text{ eV} \qquad (5)$$

$$\rightarrow ScO^+ + 2D - 2.53 \pm 0.06 \text{ eV} \qquad (6)$$

are observed in the reaction of $Sc^+ + D_2O$. Figure 1 shows the cross sections for interaction of D_2O with Sc^+ ions formed in the flow tube. As discussed above, these source conditions are believed to produce ground state a^3D ions. At low energies, formation of ScO^+ is the dominant process and increases with decreasing kinetic energy. This identifies this cross section feature with the exothermic dehydrogenation reaction 5. The ScO^+ cross section also has a feature at high energy, which can be modeled with eq 2. The threshold obtained, 2.55 ± 0.23 eV (Table 3), is in good agreement with the thermodynamic threshold for reaction 6, 2.53 ± 0.06 eV. This confirms that the ScO^+ observed at high energy is formed in reaction 6, a process that must correspond to decomposition of the $ScOD^+$ product by D atom loss.

The cross section for ScD^+ rises from energies comparable to the thermodynamic threshold for reaction 3. Analysis of the cross section for reaction 3 with eq 2 yields the optimum parameters listed in Table 3. The measured threshold, 2.83 ± 0.08 eV, is in excellent agreement with the thermodynamic value of 2.74 ± 0.09 eV. This is a further indication that there is no

TABLE 3: Summary of Parameters of Eq 2 Used To Model Reaction Cross Sections[a]

reaction	σ_0	n	E_T, eV[b]
$Sc^+(FT) + D_2O \rightarrow ScD^+ + OD$	2.4(0.4)	1.3(0.1)	2.83(0.08)
$\rightarrow ScOD^+ + D$[c]	0.31(0.04)	1.0(0.1)	≡0.04
	0.66(0.16)	1.9(0.1)	0.69(0.11)
$\rightarrow ScO^+ + 2D$	2.1(0.4)	1.2(0.1)	2.55(0.23)
$Ti^+(FT) + D_2O \rightarrow TiD^+ + OD$	1.8(0.2)	1.2(0.1)	2.88(0.05)
$\rightarrow TiOD^+ + D$[c]	0.07(0.02)	0.8(0.2)	0.31(0.04)
	0.39(0.11)	2.1(0.3)	0.78(0.15)
$\rightarrow TiO^+ + 2D$	1.3(0.1)	0.8(0.1)	2.73(0.06)
$Ti^+(SI) \rightarrow D_2O \rightarrow TiD^+ + OD$	1.4(0.2)	1.5(0.2)	2.79(0.12)
$\rightarrow TiO^+ + 2D$	0.72(0.10)	1.1(0.1)	2.61(0.06)
$Ti^+(EI) \rightarrow D_2O \rightarrow TiD^+ + OD$	1.1(0.2)	2.0(0.1)	2.30(0.13)
$\rightarrow TiO^+ + 2D$	0.64(0.08)	1.4(0.1)	2.13(0.05)

[a] Uncertainties of one standard deviation are in parentheses. [b] For FT data, the E_T value equals E_0. For SI and EI data, the E_T value reported corresponds to $E_0 - E_{el}$; see text. [c] Fitting parameters for low- and high-energy features, respectively; see text.

appreciable electronic excitation in the Sc^+ ions. ScD^+ is the dominant product at high energy, typical behavior for the reaction of atomic metal ions with H- and D-containing polyatomic molecules.[11,30] This is because angular momentum constraints restrict the formation of the $ScOD^+ + D$ channel (which has a reduced mass of 1.95 amu, much smaller than that of the reactants, 13.86 amu) relative to the $ScD^+ + OD$ channel (where the reduced mass of 13.02 amu is comparable to that of the reactants). This is an effect that we have discussed in detail previously.[31]

The cross section for formation of $ScOD^+$ in reaction 4 rises with increasing energy but is nonzero at our lowest energies of ~0.02 eV and shows a small plateau below ~0.6 eV (Figure 1). The $ScOD^+$ cross section reaches a maximum near the onsets of the ScD^+ cross section and the endothermic part of the ScO^+ cross section, while the total cross section is a smooth function of energy. This behavior is a clear indication that reaction 4 competes directly with reactions 3 and 6. Analysis of the cross section data for $ScOD^+$ is difficult because of the complex behavior with energy. However, if E_0 is held at the thermodynamic value for reaction 4, 0.04 ± 0.09 eV, the low-energy feature of $ScOD^+$ cross section can be modeled with eq 2. To reproduce this cross section at higher energies, the model for the low-energy portion of the data must be added together with a model having a threshold of 0.69 ± 0.11 eV (Table 3). This suggests that there is another pathway to form $ScOD^+ + D$ products.

$Ti^+(a^4F) + D_2O$. Three ionic products, formed in reactions 7–10,

$$Ti^+ + D_2O \rightarrow TiD^+ + OD - 2.87 \pm 0.11 \text{ eV} \quad (7)$$

$$\rightarrow TiOD^+ + D - 0.39 \pm 0.12 \text{ eV} \quad (8)$$

$$\rightarrow TiO^+ + D_2 + 1.77 \pm 0.06 \text{ eV} \quad (9)$$

$$\rightarrow TiO^+ + 2D - 2.79 \pm 0.06 \text{ eV} \quad (10)$$

are observed in the reaction of $Ti^+ + D_2O$. Figure 2 shows the cross sections for interaction of D_2O with ground state $Ti^+(a^4F)$ ions formed in the flow tube. The reaction of $Ti^+(a^4F)$ with D_2O is very similar to that of $Sc^+(a^3D)$ with D_2O shown in Figure 1. Again, formation of metal oxide, TiO^+, is the dominant process at low energy and corresponds to the exothermic reaction 9. The analysis of the high-energy feature of the TiO^+ cross section yields a threshold of 2.73 ± 0.06 eV (Table 3), confirming that this high-energy feature corresponds to reaction 10.

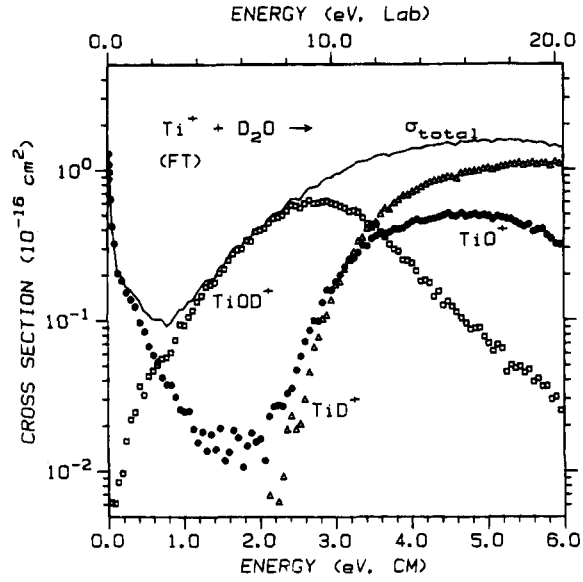

Figure 2. Variation of product cross sections for reaction of D_2O with Ti^+ produced in the flow tube (FT) source as a function of translational energy in the center-of-mass frame (lower scale) and laboratory frame (upper scale). The solid line is the sum of the cross sections for all products.

The TiD^+ product is dominant at high energy for the reasons discussed above for ScD^+. The cross section of TiD^+ has an apparent onset below the thermodynamic threshold for reaction 7, but this is because of the experimental energy distributions. Analysis of the cross section data for reaction 7 with eq 2 yields a threshold of 2.88 ± 0.05 eV, in excellent agreement with the thermodynamic value, 2.87 ± 0.11 eV. This is consistent with a Ti^+ beam that is largely in its a^4F ground state.

The cross section for $TiOD^+$ shows a maximum near the onsets of the TiD^+ cross section and the endothermic part of the TiO^+ cross section, and the total cross section is a smooth function of energy. This indicates that reaction 8 competes directly with reactions 7 and 10. The cross section for reaction 8 cannot be reproduced with eq 2 over the entire experimental energy region studied. As in the scandium system, we believe that the cross section of $TiOD^+$ has two features although this is not as apparent as it is for the $ScOD^+$ cross section. We find that the cross section can be reproduced nicely if we break the data into a low-energy part below ~0.8 eV and a high-energy part above this energy. For the low-energy part, the analysis of the data using eq 2 gives a threshold of 0.31 ± 0.04 eV, within experimental error of the thermodynamic threshold for reaction 8, 0.39 ± 0.12 eV. Analysis of the high-energy part of the cross section for $TiOD^+$ yields a threshold of 0.78 ± 0.15 eV, although the accuracy of this threshold is not definitive because it depends critically on the cross section model used for the lower-energy pathway.

The qualitative features of the cross sections for reaction of D_2O with $Sc^+(a^3D)$ and $Ti^+(a^4F)$ are similar to those previously reported for the reaction of V^+ with D_2O[6] and the interactions of Sc^+, Ti^+, and V^+ with ammonia[10,32] and methane.[11,12,31] In these latter systems, the reactivity is dominated by the dehydrogenation channels at low energy (an exothermic reaction for ammonia and endothermic for methane) and by formation of MH^+ at high energies. Competition between formation of MH^+ and MNH_2^+ or MCH_3^+ (the isoelectronic analogues of MOD^+) is also observed.

Electronic State Dependence. In order to quantitatively assess the electronic state effects on the reactivity for the reaction

of Ti^+ with D_2O, we have generated Ti^+ in three different sources: the flow tube (FT), surface ionization (SI), and electron impact (EI) sources. In the following sections, we compare how the means of ion production change the data for each individual product channel.

TiD^+. Figure 3a shows the $TiD^+ + OD$ cross section data when Ti^+ is produced in the FT, SI, and EI sources. The FT and SI cross sections rise from nearly the same threshold. Analysis of the SI data with eq 2 gives a threshold $E_T = 2.79 \pm 0.12$ eV (Table 3), which is not significantly different than the threshold of 2.88 ± 0.05 eV measured for the FT data. This good agreement between FT and SI measured thresholds indicates that the contribution to the TiD^+(SI) cross section from the a^2F and other higher-lying excited states (Table 1) is negligible; otherwise, the threshold measured for the SI data would be shifted to lower energy. This threshold agreement cannot definitively eliminate a possible contribution to the TiD^+-(SI) cross section from the first excited b^4F state (35.6% of the beam), because its energy (0.135 eV) is close to the ground a^4F state. However, we note that the magnitude of the SI cross section is $67 \pm 6\%$ of the FT cross section below ~4.2 eV, a percentage that matches the population of the ground a^4F state ions in the SI beam, 62.5% at 2200 K (Table 1). This suggests that the SI cross section for TiD^+ below 4.2 eV is due primarily to reaction of ground a^4F state, which is much more reactive than the first excited b^4F state with respect to forming $TiD^+ + OD$ products below 4.2 eV. Above this energy, the SI cross section approaches and then surpasses the FT cross section. This observation suggests that the b^4F state may react with D_2O to form TiD^+ through a high-energy pathway with an apparent onset near 4.2 eV.

Figure 3a also shows that the TiD^+(EI) cross section is larger than the FT and SI data and begins to rise at lower energies. Analysis of the EI cross section with eq 2 gives a threshold of $E_T = 2.30 \pm 0.13$ eV (Table 3). Comparison of this E_T value with the thermodynamic threshold measured from reaction of the a^4F ground state yields $E_{el} = 0.58 \pm 0.14$ eV, which is only consistent with the excitation energy of the a^2F excited state, 0.593 eV (Table 1). The larger cross section and E_{el} value suggest that the a^2F excited state contributes considerably to the reactivity in the EI data. This contribution is assessed more quantitatively below.

TiO^+. Figure 3b shows the FT, SI, and EI cross sections for reactions 9 and 10. Below 1 eV, the SI data are larger than the FT data by a factor of 4 ± 1, indicating a contribution to the TiO^+(SI) cross section from ions in excited states. The EI data in turn are larger than the SI data, consistent with a population increase of high-lying excited states in the EI beam (Table 1).

For the high-energy portion of the TiO^+ cross section, analyses of the FT and SI data yield thresholds of 2.73 ± 0.06 and 2.61 ± 0.06 eV, respectively, which are consistent with each other within the combined experiment errors. This indicates no significant contribution to the high-energy portion of the SI cross section from a^2F and other higher-lying excited states. Also, the high-energy portion of the SI data has a magnitude that is $64 \pm 4\%$ of FT data, consistent with the 62.5% of ground state ions produced in the SI source. This result implies that the b^4F state is relatively unreactive. The threshold for the high-energy portion of the EI data is 2.13 ± 0.05 eV, 0.60 ± 0.08 eV lower than that of the FT data, and consistent with reaction of $Ti^+(a^2F)$ excited state ions.

$TiOD^+$. Figure 3c shows the cross sections for formation of $TiOD^+ + D$, reaction 8, when Ti^+ is produced in the FT, SI, and EI sources. The SI data are larger than the FT data at low energies, but the magnitude is $55 \pm 5\%$ of the FT data near the peak of the data. The relative magnitude at higher energies is

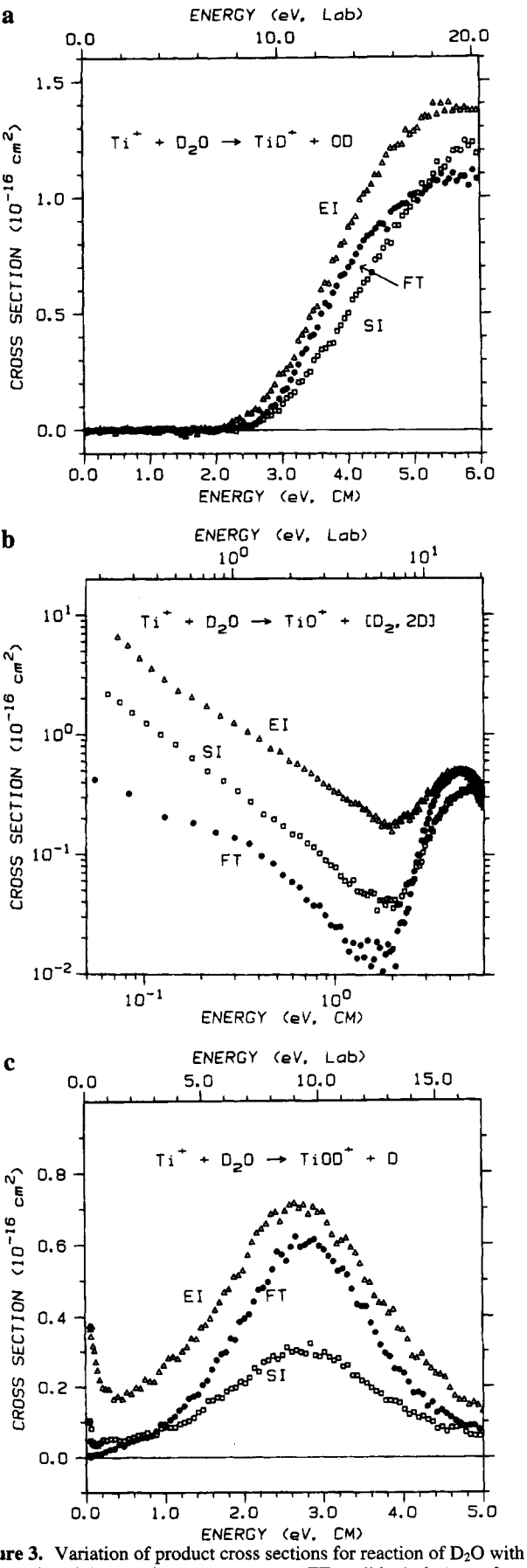

Figure 3. Variation of product cross sections for reaction of D_2O with Ti^+ produced in the flow tube source (FT, solid circles), surface ionization source (SI, open squares), and 30 eV electron impact source (EI, open triangles) as a function of translational energy in the center-of-mass frame (lower scale) and laboratory frame (upper scale). Part a shows results for the $TiD^+ + D$ product channel; part b, the $TiO^+ + [D_2, 2D]$ product channel; and part c, the $TiOD^+ + D$ product channel.

roughly consistent with the 62.5% population of the a^4F ground state in the SI beam (Table 1), suggesting again that the b^4F first excited state is relatively unreactive. The difference in shapes between the FT and SI data at low energies is consistent with the appearance of an exothermic reaction channel in the SI data. This increase in the SI cross section for $TiOD^+ + D$ must be due largely to reaction of a^2F and higher-lying excited states, because reaction of the first excited state (b^4F) is endothermic by 0.25 ± 0.12 eV.

The EI cross section for $TiOD^+ + D$ is larger than the FT and SI data and shows behavior characteristic of both an endothermic and exothermic process. The exothermic reaction must be due to reaction of a^2F and higher-lying excited states because lower-lying states do not have enough energy to react exothermically. The exothermic portion of the EI cross section is about 6 times that observed in the SI cross section. This roughly matches the population ratio of $Ti^+(a^2F)$ and higher-energy states produced in the SI (~2%) and EI sources (Table 1).

State-Specific Cross Sections. Although the FT results are believed to correspond directly to cross sections for reaction of $Ti^+(a^4F)$, it would be useful to estimate cross section for other electronic states of Ti^+. The results discussed above show that the b^4F state is relatively unreactive, and hence it makes no appreciable contributions to the observed cross sections except in the case of the $TiD^+ + OD$ reaction channel. Higher-lying electronic states, in particular the a^2F state, are much more reactive and extraction of cross sections for these states is possible. Conceivably, this could be accomplished by correcting the SI data for the a^4F state contributions, but the result has a large uncertainty because the population of the a^2F state in the SI beam is small (Table 1). The a^2F contribution increases substantially for the EI beam, but here the absolute fraction of ground state a^4F is not known with certainty. As mentioned in the Experimental Section, we have quantitatively assessed the sum of the a^4F and b^4F state populations (Table 1) but have no accurate information about the individual populations for Ti^+ produced in our EI source. To deduce a conservative estimate of the state-specific reactions cross sections, we assume two limiting sets of state populations for the Ti^+ beam produced by 30 eV EI. For both sets, we adopt 14 ± 6% as the population of a^2F state,[10] a value that encompasses the upper limit of Kemper and Bowers and our lower value of 9 ± 3%.[11] For the sum of the populations of the a^4F and b^4F states, we adopt 80% in accord with our previous results[11] and those of Kemper and Bowers.[25] The only difference between the two sets of populations is whether the population of the b^4F state is taken as 0%, a minimum value in accord with Kemper and Bowers, or 40%, a reasonable maximum value because it equally populates the two closely spaced a^4F and b^4F states which have identical electronic degeneracies. The remaining 6 ± 6% of the population needed to bring the total to 100% is assumed to be in high-lying and unreactive states.

Given these assumptions, the TiD^+ cross section for the b^4F state is obtained by scaling the $Ti^+(FT,a^4F)$ cross section by its population in the SI beam (62.5%) and subtracting this from the SI data. The remaining portion of the SI data, which is due primarily to reaction of the 35.6% of the ions in the b^4F state, is scaled to 100%. There are contributions from ≤2% of the a^2F and other higher-lying excited state ions, but these are small and ignored. The a^2F excited state cross section for TiD^+ is obtained by subtracting 80 or 40% of the a^4F cross section (FT data) and 0 or 40% of the b^4F cross section from the EI data and scaling the remainder from 14% to 100%. The cross sections for TiO^+ and $TiOD^+$ associated with the a^2F state are obtained by scaling the corresponding FT a^4F cross sections by

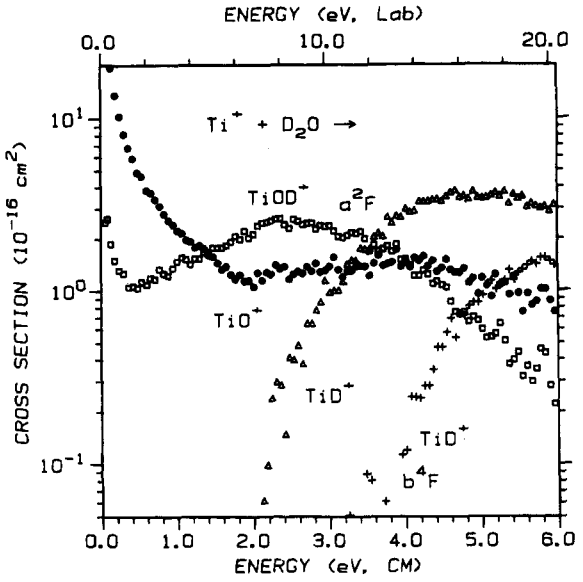

Figure 4. State-specific cross sections for the reaction of D_2O with Ti^+ as a function of translational energy in the laboratory (upper axis) and center-of-mass frame (lower axis). Results for reaction of $Ti^+(a^2F)$ derived as discussed in the text are shown by circles (TiO^+), squares ($TiOD^+$), and triangles (TiD^+). Results for reaction of $Ti^+(b^4F)$ to form TiD^+ are shown by plus symbols.

80 or 40% and subtracting these from the EI data. The remaining portion of the EI data is due primarily to reaction of 14 ± 6% of the ions in the a^2F state and possibly a small fraction of the ions in higher-lying states. Thus, dividing the remainder by 0.14 yields an estimate of the a^2F cross sections, the dominant state in the EI beam. We are unable to estimate the TiO^+ and $TiOD^+$ cross sections for the b^4F state because it is relatively unreactive and makes no significant contributions to the SI or EI cross sections of these two product ions, as noted above.

The average of the upper and lower limits for the a^2F cross sections for the TiD^+, TiO^+, and $TiOD^+$ product ions derived in this manner are shown in Figure 4, together with the b^4F cross section for the TiD^+ product ion. The absolute uncertainties in the a^2F cross sections are appreciable due to the various assumptions about the absolute populations of the electronic states and because of small but uncharacterized contributions from the b^4F and states above the a^2F. These uncertainties primarily influence the magnitudes of the derived a^2F cross sections but not their shapes. A conservative estimate of the errors in the a^2F cross sections is plus or minus a factor of 2.

Even though the absolute uncertainty in the a^2F state cross sections is considerable, this state is clearly much more reactive than the ground a^4F state (Figure 2) for all three reaction channels. For the endothermic portions of all three cross sections, the a^2F state is 2−7 times more reactive than the a^4F ground state, while for the exothermic formation of $TiO^+ + D_2$ products in reaction 9, the a^2F state is about 70 times more reactive than the a^4F. Modeling of the a^2F cross sections with eq 2 yields thresholds of E_T = 2.28 ± 0.13 eV for the TiD^+ cross section and 2.17 ± 0.09 eV for the endothermic portion of the TiO^+ cross section. Comparisons of these values with the thresholds for reactions 7 and 10 measured from FT data (Table 3) yield E_{el} of 0.60 ± 0.14 and 0.56 ± 0.11 eV, respectively, in good agreement with the electronic excitation energy of a^2F state, 0.593 eV. This agreement supports our assumption that the dominant reactive state in the EI generated beam is the a^2F state. Contributions from higher-lying states are apparently small, because of either their small populations or lower reactivities.

For $TiOD^+$, reaction of $Ti^+(a^2F)$ with D_2O to form $TiOD^+ + D$ should be exothermic by 0.20 ± 0.12 eV, in agreement

with the cross section behavior shown in Figure 4. However, there is also an endothermic feature in the a^2F cross section for $TiOD^+$. We have carefully checked that this is not an artifact of the means used to extract this state-specific cross section. Indeed, this bimodal cross section is analogous to that obtained for $V^+(a^3F) + D_2O \rightarrow VOD^+ + D$.[6] This cross section suggests that the $Ti^+(a^2F)$ state reacts with D_2O to form $TiOD^+ + D$ products in both an exothermic barrierless pathway at low energy and a high-energy pathway. Analysis of the endothermic portion of the a^2F cross section gives a threshold of $E_T = 0.46 \pm 0.04$ eV.

Modelling of the b^4F cross section for TiD^+ formation with eq 2 yields a threshold of ~4.3 eV. This is much higher than the thermodynamic threshold of 2.73 ± 0.11 eV for this state-specific reaction. This is consistent with the relative inertness of this state compared to the other electronic states of Ti^+.

Reaction Efficiency and Rate Constants. The overall efficiencies of these reactions can be estimated by comparing our total state-specific cross sections for $Sc^+(a^3D)$, $Ti^+(a^4F)$, and $Ti^+(a^2F)$ with the collision cross sections calculated by using an ion-locked dipole (LD) model, $\sigma_{LD} = \pi e(2\alpha/E)^{1/2} + \pi e(\mu_D/E)$,[33] where the first term is the Langevin–Gioumousis–Stevenson cross section for collisions with polarizable molecules,[34] α and μ_D are the polarizability and the electric dipole moment of the neutral reactant molecule (1.45 Å^3 and 1.84 D for H_2O, respectively[35]), and e is the charge on the electron. Although this model provides only an upper limit to the collision cross section for the ion–molecule reactions in which the neutral molecules has an appreciable dipole moment, we find that it accurately reproduces the energy dependence of our experimental cross sections. Below ~0.5 eV, the a^4F and a^2F states of Ti^+ react with $0.15 \pm 0.07\%$ and $10 \pm 3\%$ efficiencies, respectively, while $Sc^+(a^3D)$ has a $0.7 \pm 0.2\%$ reaction efficiency. A more realistic estimate of the cross section for ion–polar molecule collisions comes from results of Su,[36] who has calculated rate constants for over 100 systems by using a trajectory method. The results of these calculations can be reproduced in terms of a parametrized model that depends only on α, μ_D, E and the rotational temperature. The difference between this model cross section and σ_{LD} is energy dependent such that Su's model is about 60% σ_{LD} at an energy of 0.04 eV ($= 3k_BT/2$ at 300 K); they are nearly the same near an energy of about 0.5 eV, where Su's model again becomes increasingly smaller than σ_{LD} as the energy increases further. Comparison of our results with those of Su's model over the energy region of ~0.04 to ~0.5 eV gives average reaction efficiencies that are about 12% larger than those obtained from comparison with the ion-locked dipole model above.

Our experimental cross sections can be converted to phenomenological rate constants by $k(\langle E \rangle) = v\sigma(E)$ where $v = (2E/\mu)^{1/2}$, μ is the reduced mass of the reactants, $\langle E \rangle = E + (3/2)\gamma k_BT$, $\gamma = M/(M + m)$, and T is the temperature of the reactant gas (305 K).[16] For the present results, we determine 300 K rate constants of $(3 \pm 1) \times 10^{-12}$, $(2 \pm 1) \times 10^{-10}$, and $(1.3 \pm 0.4) \times 10^{-11}$ cm^3 s^{-1} for the reactions of D_2O with $Ti^+(a^4F)$, $Ti^+(a^2F)$, and $Sc^+(a^3D)$, respectively. The uncertainties listed are conservative estimates that include variations among different data sets and errors in the absolute cross sections used to derive these rate constants. Our value for the reaction of $Ti^+(a^4F)$ is much smaller than the $(1.00 \pm 0.02) \times 10^{-10}$ cm^3 s^{-1} value reported by Castleman and co-workers.[13] There are two likely explanations for this discrepancy. One is that their Ti^+ beam contains appreciable amounts of excited a^2F state because the He buffer gas does not effectively quench this state to the a^4F ground state, as shown by Kemper and Bowers in their ion chromatography study.[25] This possibility is supported by the fact that the rate constant of Castleman and co-workers' is comparable to our value for the a^2F excited state. A second explanation is that their water sample may have O_2 contamination, which is known to react very efficiently with Sc^+, Ti^+, and V^+ to form MO^+ ions.[27] This O_2 contamination problem had been noted in our previous study of the reaction of V^+ with D_2O[6] and was also observed for the Sc^+ and Ti^+ systems if the D_2O was not purged with dry N_2 before use.

Discussion

Potential Energy Barriers or Isomers. As noted above, the cross sections for $MOD^+ + D$ formation from $Sc^+(a^3D)$, $Ti^+(a^4F)$, and $Ti^+(a^2F)$ ions exhibit two features: a small feature having a threshold 0.5–0.7 eV lower than a larger feature at higher energies (Figures 1, 2, and 4). One possible explanation for these two features is that an $D-M^+-O$ isomer is formed. Tilson and Harrison[15] have calculated that $H-Sc^+-O$ is less stable than Sc^+-OH by 4.0 eV, a much larger difference than the energetic difference observed for the two features here. The $D-Ti^+-O$ isomer is probably more stable relative to Ti^+-OD than in the scandium case, because Ti^+ has enough electrons to form a covalent M^+-D bond and a covalent $M^+=O$ double bond, while Sc^+ does not. Nevertheless, it seems unlikely that the $D-Ti^+-O$ would be close enough in energy to the Ti^+-OD isomer to explain the two features in the experimental cross section.

Another possible explanation for the two features observed is that the small feature at low energy is due to excited state metal ions in the beam. This possibility is ruled out in the titanium system where state-specific cross sections are extracted. In the scandium system, the first excited state (a^1D, 0.32 eV) might account for the low-energy feature of $ScOD^+$, but the similarity in the $ScOD^+$ and $TiOD^+$ cross section discounts this possibility. The most plausible explanation for the two features observed in the MOD^+ cross section is that reactions 4 and 8 have two different pathways: an inefficient one beginning at the thermodynamic threshold and a more efficient one beginning at higher energy. A similar conclusion was reached for the reaction $V^+(a^3F) + D_2O \rightarrow VOD^+ + D$.[6] Possible pathways are discussed further below.

Reaction Mechanism. As discussed in detail in our previous studies,[1,3,6] there are two reasonable mechanisms for the interaction of M^+ with D_2O: M^+ insertion into a $D-OD$ bond to form a $D-M^+-OD$ intermediate, **I**, or direct abstraction of the D atom or the OD group from D_2O. Formation of $MD^+ + OD$ and $MOD^+ + D$ can occur from intermediate **I** by simple M^+-OD or M^+-D bond fission, respectively. The insertion mechanism explains the strong competition observed between MD^+ and MOD^+ in both the Sc^+ and Ti^+ systems. Similarly, we have used the insertion mechanism to account for the strong competition between formation of MOD^+ and MD^+ observed in the reaction D_2O with Co^+,[1] Fe^+,[3] and V^+.[6] In the reaction of Sc^+ and Ti^+ with ND_3[10] and CH_4,[11,12] we used analogous insertion intermediates, $D-M^+-ND_2$ and $H-M^+-CH_3$, to explain the strong competition between MD^+ and MND_2^+ and between MH^+ and MCH_3^+.

As noted in the introduction, the formation of $MO^+ + D_2$ products, the dehydrogenation channels corresponding to reactions 5 and 9, can proceed from intermediate **I** by forming a four-centered transition state or by forming D_2M^+-O and then eliminating D_2. A molecular orbital analysis of these processes has led us to conclude that the four-centered transition state is the likely mechanism in the case of V^+.[6] In addition, we note that because Sc^+ has only two valence electrons, it cannot form a H_2Sc^+-O intermediate unless one of the bonds is not covalent (making it much less stable). Hence, no such intermediate is

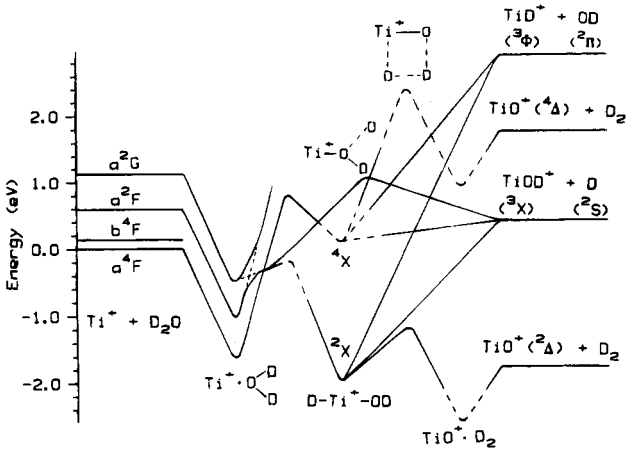

Figure 5. Semiquantitative potential energy surfaces for the reaction of Ti^+ with D_2O to form TiD^+, TiO^+, and $TiOD^+$. Short dashed lines indicate an avoided surface crossing. Long dashed lines indicate that no experimental information is available to allow a quantitative estimate of the energy. For simplicity, $Ti^+(a^2D)$ and the surface evolving from $Ti^+(b^4F)$ are not shown.

included in Tilson and Harrison's calculations,[15] although they do calculate properties of the (H_2)·Sc^+−O species that would be formed in the exit channel for hydrogen elimination by either mechanism. Because the reaction cross sections for the Sc^+, Ti^+, and V^+ systems are so similar, it seems unlikely that different reaction pathways are operative in the different systems.

Potential Energy Surfaces. Figure 5 shows qualitative potential energy surfaces for the $Ti^+ + D_2O$ reaction system. The analogous diagram for the Sc^+ system is qualitatively similar. The initial interaction is attractive because of the long-range ion−dipole potential. Thus, there is well corresponding to the Ti^+·OD_2 complex, which has a $^4B_1(4s^13d\pi^13d\delta^1)$ ground state according to theoretical calculations.[37] The energy of the ground state Ti^+·OD_2 complex is taken from the Ti^+-OH_2 bond energy, 1.60 ± 0.06 eV[38] (Table 2). All Ti^+ states are assumed to bind D_2O with comparable bond strengths. As the Ti^+ ion approaches D_2O closely, it inserts into the O−D bond of D_2O to form intermediate **I**. On the basis of the bond additivity assumption that $D_0(DOM^+-D) \approx D_0(M^+-D)$ (Table 2), the energy of the D−Ti^+−OD ground state intermediate is estimated to be 1.95 ± 0.16 eV below the $Ti^+ + D_2O$ asymptote. For comparison, Tilson and Harrison[15] calculate that H−Sc^+−OH is 1.73 eV more stable than $Sc^+ + H_2O$, but their calculation of the Sc^+−OH bond strength is 0.5 eV lower than our experimental value (Table 2). Correcting for this difference yields an estimated energy for H−Sc^+−OH of 2.23 eV below $Sc^+ + H_2O$, in reasonable agreement with the bond additivity estimate of 2.43 ± 0.13 eV (Table 2).

The oxidative addition of a covalent σ bond to M^+ is believed to be most facile when the metal has an empty 4s orbital to accept the pair of electrons in the covalent bond and when it has a pair of $3d\pi$ electrons that have the proper symmetry to donate into the antibonding orbital of the bond to be broken.[8] In the present study, the lowest electronic state for Sc^+ having such an electronic configuration is the $b^1D(3d^2)$ state, and the lowest for Ti^+ is the $a^2G(3d^3)$. Moreover, if the M−D and M−OD bonds in the insertion intermediate **I** are covalent, then the D−Sc^+−OD intermediate has a singlet spin ground state and the D−Ti^+−OD intermediate has a doublet spin ground state. This argument is consistent with Tilson and Harrison's calculation[15] that H−Sc^+−OH has ^1A ground state and with results of Rosi et al.,[39] who calculate that the analogous Sc-$(CH_3)_2^+$ and Ti$(CH_3)_2^+$ species have singlet and doublet spin ground states, respectively. Given this information, the Ti^+-$(a^2G,3d^3)$ state *diabatically* correlates with the ground state of D−Ti^+−OD. The surfaces corresponding to this state should undergo avoided crossings with those evolving from the Ti^+-$(a^2F,4s3d^2)$ and $Ti^+(a^2D,4s3d^2)$ asymptotes, and hence Figure 5 shows that the a^2F state *adiabatically* correlates with the ground state of D−Ti^+−OD. The surfaces evolving from the ground state $Ti^+(a^4F) + D_2O$ asymptote must correlate with an excited quartet state of the D−Ti^+−OD insertion intermediate. In the scandium system, the ground state of D−Sc^+−OD correlates *diabatically* with $Sc^+(b^1D,3d^2) + D_2O$ and *adiabatically* with the $Sc^+(a^1D,4s3d^1)$ first excited state, while the Sc^+-(a^3D) ground state correlates with an excited triplet state of the D−Sc^+−OD intermediate.

Both the low-spin ground state and high-spin excited state of the D−M^+−OD intermediates can decompose to form ground state $MD^+ + OD$ (reactions 3 and 7) and $MOD^+ + D$ (reactions 4 and 8) by simply breaking the M−OD or M−D bond. These reactions conserve electron spin because their neutral products, D and OD, have doublet spin, while their ionic products, ScD^+ and $ScOD^+$, have doublet spin and TiD^+ and $TiOD^+$ have triplet spin.[40]

As shown in Figure 5, the doublet and quartet potential energy surfaces for the $Ti^+ + D_2O$ reaction system lead to $TiO^+(^2\Delta) + D_2$ and $TiO^+(^4\Delta) + D_2$ products, respectively. Similarly, in the scandium system, the singlet and triplet potential energy surfaces lead to the $ScO^+(^3\Delta) + D_2$ and $ScO^+(^1\Sigma^+) + D_2$ products, respectively. The high-spin states of both ScO^+ and TiO^+ have been calculated to lie higher than the low-spin ground states by about 3.5 eV.[15,41] In both systems, we observe that high-spin ground state metal ions react with D_2O to form $MO^+ + D_2$ in exothermic processes, indicating that the lowest-energy surfaces leading to ground state $MO^+ + D_2$ products have no barriers that are higher than the energies of the ground state $M^+ + D_2O$ reactants. The efficiencies of these reactions decrease from 0.7% for $M^+ = Sc^+(a^3D)$ to 0.15% for $M^+ = Ti^+(a^4F)$ to 0% for $M^+ = V^+(a^5D)$,[6] consistent with the relative efficiencies observed for the reverse reaction.[5] These observations help confirm the hypothesis discussed in the Introduction for these systems. The observation that these dehydrogenation reactions are exothermic indicates that the high-spin, ground state reactants must couple to the low-spin surfaces that lead to ground state $MO^+ + D_2$ products, because formation of high-spin $MO^+ + D_2$ products is strongly endothermic in both systems. The spin-forbidden nature of these reactions explains the low efficiencies for the high-spin $Sc^+(a^3D)$ and $Ti^+(a^4F)$ states compared to the 10% efficiency observed for the low-spin $Ti^+(a^2F)$ state, which can form ground state $MO^+ + D_2$ products in a spin-allowed process.

The observation that the low-spin a^2F state also forms the $TiOD^+ + D$ and $TiD^+ + OD$ products more efficiently than the high-spin a^4F state (even though these products can be formed in spin-allowed processes from either state) can be explained as long as the reactions of both states preferentially proceed via the low-spin ground state of intermediate **I**. Presumably, $Ti^+(b^4F)$ is less reactive than $Ti^+(a^4F)$ because it correlates with a more repulsive surface (and thus couples with the low-spin surfaces less efficiently) and a high-spin intermediate even higher in energy than that shown in Figure 5. Thus, the only appreciable reactivity observed here is formation of TiD^+ at elevated energies in what is probably a direct abstraction reaction.

It is interesting to note that we do not observe any obvious features in the MO^+ cross sections that can be attributed to spin-allowed formation of high-spin $MO^+ + D_2$. These could appear at kinetic energies of about 1.4 and 1.8 eV in the scandium and titanium systems, respectively. We have observed such spin-

allowed, but thermodynamically disfavored, processes in the reaction of $V^+ + CO_2 \rightarrow VO^+ + CO$.[42] In the present systems, it seems likely that this type of process is suppressed by competition with formation of $MOD^+ + D$. This is also a spin-allowed process that is thermodynamically (endothermicities of 0.04 and 0.39 eV, respectively) favored over the high-spin $MO^+ + D_2$ channel and should be kinetically favored as well, because it can occur by simple bond fission while dehydrogenation requires a tight transition state.

Finally, we want to explain the observation of two features in the cross sections for the $MOD^+ + D$ product channel observed for $Sc^+(a^3D)$, $Ti^+(a^4F)$, and $Ti^+(a^2F)$. A similar observation was made for this product channel in the reaction of D_2O with low-spin excited $V^+(a^3F)$[6], and such bimodal behavior has also been observed for the reactions of metal ions with methanol and methyl chloride.[2,43,44] In these cases, we have attributed the bimodal behavior to an insertion mechanism at low energies and a more direct mechanism at higher energies. In the reaction of $Ti^+(a^2F) + D_2O$, the direct mechanism corresponds to cleavage of an O−D bond in the Ti^+-OD_2 intermediate. A qualitative explanation for the origin of a barrier for this process can be seen by considering the molecular orbitals involved in the reverse process, approach of a deuterium atom to $TiOD^+$. The $TiOD^+$ molecule is likely to have a triplet ground state[40] with the two unpaired electrons located primarily on the titanium atom in nonbonding orbitals. Thus, addition of a deuterium atom to the titanium end of $TiOD^+$ (which forms **I**) should lead to an attractive covalent interaction (Figure 5). Addition of a deuterium atom to the oxygen atom in $TiOD^+$ (which forms the Ti^+-OD_2 intermediate) should be repulsive because all of the orbitals on the oxygen atom are filled. This repulsive interaction could lead to the barrier observed experimentally and is shown in Figure 5.

For the reaction of D_2O with the $Sc^+(a^3D)$ and $Ti^+(a^4F)$ ground states, the two features in the $MOD^+ + D$ product cross sections can now be explained by coupling to the low-spin surface and then allowing the products to form by the two mechanisms postulated for the a^2F state. Another plausible explanation in the case of the ground states (but not for the excited state) is that the small feature at low energies corresponds to inefficient coupling to the low-spin surface to form the ground state of intermediate **I** followed by formation of the products at their thermodynamic threshold. The larger feature at higher energy could then result from the spin-allowed reaction along the high-spin surface, such that the derived thresholds for the high-energy features (0.68 ± 0.11 and 0.76 ± 0.15 eV for the scandium and titanium system, respectively) could represent the barrier heights between the $M^+ \cdot OD_2$ complexes and the high-spin states of intermediates **I**.

Acknowledgment. This work is supported by the National Science Foundation, Grant CHE-9221241. The authors thank M. Knowles for helping to acquire some of the data.

References and Notes

(1) Chen, Y.-M.; Clemmer, D. E., Armentrout, P. B. *J. Am. Chem. Soc.* **1994**, *116*, 7815.

(2) Chen, Y.-M.; Clemmer, D. E.; Armentrout, P. B. Manuscript in preparation.

(3) Clemmer, D. E.; Chen, Y.-M.; Khan, F. A.; Armentrout, P. B. *J. Phys. Chem.* **1994**, *98*, 6522.

(4) Schröder, D.; Fiedler, A.; Ryan, M. F.; Schwarz, H. *J. Phys. Chem.* **1994**, *98*, 68.

(5) Clemmer, D. E.; Aristov, N.; Armentrout, P. B. *J. Phys. Chem.* **1993**, *97*, 544.

(6) Clemmer, D. E.; Chen, Y.-M.; Aristov, N.; Armentrout, P. B. *J. Phys. Chem.* **1994**, *98*, 7538.

(7) Fiedler, A.; Schröder, D.; Shaik, S.; Schwarz, H. *J. Am. Chem. Soc.*, submitted for publication.

(8) Armentrout, P. B. In *Gas Phase Inorganic Chemistry*, Russell, D. H., Ed.; Plenum: New York, 1989; p 1. Armentrout P. B.; Beauchamp, J. L. *Acc. Chem. Res.* **1989**, *22*, 315. Armentrout, P. B. In *Selective Hydrocarbon Activation Principles and Progress*: Davies, J. A., Watson, P. L., Liebman, J. F., Greenberg, A., Eds.; VCH: New York, 1990; p 467. Armentrout, P. B. *Science* **1991**, *251*, 175. Armentrout, P. B. *Annu. Rev. Phys. Chem.* **1990**, *41*, 313.

(9) Bent, H. A. *J. Chem. Educ.* **1966**, *43*, 170.

(10) Clemmer, D. E.; Sunderlin, L. S.; Armentrout, P. B. *J. Phys. Chem.* **1990**, *94*, 3008.

(11) Sunderlin, L. S.; Armentrout, P. B. *J. Phys. Chem.* **1988**, *92*, 1209.

(12) Sunderlin, L. S.; Armentrout, P. B. *J. Am. Chem. Soc.* **1989**, *111*, 3845.

(13) Guo, B. C.; Kerns, K. P.; Castleman, A. W. *J. Phys. Chem.* **1992**, *96*, 4879.

(14) Buckner, S. W.; Gord, J. R.; Freiser, B. S. *J. Am. Chem. Soc.* **1988**, *110*, 6606.

(15) Tilson, J. L.; Harrison, J. F. *J. Phys. Chem.* **1991**, *95*, 5097

(16) Ervin, K. M.; Armentrout, P. B. *J. Chem. Phys.* **1985**, *83*, 166.

(17) Schultz, R. H.; Armentrout, P. B. *Int. J. Mass Spectrom. Ion Processes* **1991**, *107*, 29.

(18) Teloy, E.; Gerlich, D. *Chem. Phys.* **1974**, *4*, 417. Gerlich, D. Diplomarbeit, University of Freiburg, Federal Republic of Germany, 1971. Gerlich, D. In *State-Selected and State-to-State Ion-Molecule Reaction Dynamics. Part 1. Experiment*, Ng, C.-Y., Baer, M., Eds.; *Adv. Chem. Phys.* **1992**, *82*, 1.

(19) Chantry, P. J. *J. Chem. Phys.* **1971**, *55*, 2746.

(20) Ervin, K. M.; Armentrout, P. B. *J. Chem. Phys.* **1987**, *86*, 2659.

(21) Schultz, R. H.; Crellin, K. C.; Armentrout, P. B. *J. Am. Chem. Soc.* **1991**, *113*, 8590.

(22) van Koppen, P. A. M.; Kemper, P. R.; Bowers, M. T. *J. Am. Chem. Soc.* **1992**, *114*, 10941.

(23) Garstang, R. H. *Mon. Not. R. Astron. Soc.* **1962**, *124*, 321; personal communication.

(24) Kiser, R. W.; Dillard, J. G.; Dugger, D. L. *Adv. Chem. Ser.* **1969**, *72*, 753.

(25) Kemper, P. R.; Bowers, M. T. *J. Phys. Chem.* **1991**, *95*, 5134.

(26) Loh, S. K.; Fisher, E. R.; Lian, L.; Shultz, R. H.; Armentrout, P. B. *J. Phys. Chem.* **1989**, *93*, 3159.

(27) Fisher, E. R.; Elkind, J. L.; Clemmer, D. E.; Georgiadis, R.; Loh. S. K.; Aristov, N.; Sunderlin, L. S.; Armentrout, P. B. *J. Chem. Phys.* **1990**, *93*, 2676.

(28) Armentrout, P. B. In *Advances in Gas Phase Ion Chemistry*, Adams, N. G.; Babcock, L. M., Eds.; JAI: Greenwich, 1992; Vol. 1, p 83.

(29) Armentrout, P. B. In *Structure/Reactivity and Thermochemistry of Ions*, Ausloos, P., Lias, S. G., Eds.; Reidel: Dordrecht, 1987; p 97.

(30) Aristov, N.; Armentrout, P. B. *J. Am. Chem. Soc.* **1986**, *108*, 1806. Georgiadis, R.; Fisher, E. R.; Armentrout, P. B. *J. Am. Chem. Soc.* **1989**, *111*, 4251.

(31) Aristov, N.; Armentrout, P. B. *J. Phys. Chem.* **1987**, *91*, 6178.

(32) Clemmer, D. E.; Sunderlin, L. S.; Armentrout, P. B. *J. Phys. Chem.* **1990**, *94*, 208.

(33) Gupta, S. K.; Jones, E. G.; Harrison, A. G.; Myher, J. J. *Can. J. Chem.* **1967**, *45*, 3107.

(34) Langevin, M. P. *Ann. Chim. Phys.* **1905**, *5*, 245. Gioumousis, G.; Stevenson, D. P. *J. Chem. Phys.* **1958**, *29*, 294.

(35) Rothe, E. W.; Bernstein, R. B. *J. Chem. Phys.* **1959**, *31*, 1619.

(36) Su, T. Personal communication; *J. Chem. Phys.*, submitted.

(37) Rosi, M.; Bauschlicher, C. W. *J. Chem. Phys.* **1990**, *92*, 1876.

(38) Dalleska, N. F.; Honma, K.; Sunderlin, L. S.; Armentrout, P. B. *J. Am. Chem. Soc.* **1994**, *116*, 3519.

(39) Rosi, M.; Bauschlicher, C. W.; Langhoff, S. R.; Partridge, H. *J. Phys. Chem.* **1990**, *94*, 8656.

(40) ScH^+ and TiH^+ have $^2\Delta$ and $^3\Phi$ ground states, respectively (Pettersson, L. G. M.; Bauschlicher, C. W.; Langhoff, S. R. *J. Chem. Phys.* **1987**, *87*, 481). $ScOH^+$ has a $^2\Delta$ ground state, ref 15. If the Ti^+-OH bond has covalent character, as seems likely, $TiOH^+$ should have a triplet spin ground state like TiH^+. OD and D_2 have $^2\Pi$ and $^1\Sigma_g^+$ ground states, respectively (Huber, K. P.; Herzberg, G. *Molecular Spectra and Molecular Structure, IV. Constants of Diatomic Molecules*, Van Nostrand Reinhold: New York, 1979).

(41) Dyke, J. M.; Gravenor, B. W. J.; Josland, G. D.; Lewis, R. A.; Morris, A. *Mol. Phys.* **1984**, *53*, 465.

(42) Sievers, M. R.; Armentrout, P. B. *J. Chem. Phys.*, in press.

(43) Fisher, E. R.; Sunderlin, L. S.; Armentrout, P. B. *J. Phys. Chem.* **1989**, *93*, 7375. Fisher, E. R.; Schultz, R. H.; Armentrout, P. B. *J. Phys. Chem.* **1989**, *93*, 7382.

(44) Clemmer, D. E.; Aristov, N.; Armentrout, P. B. Unpublished results.